THE JOURNAL OF PHYSICAL CHEMISTRY C

Article

pubs.acs.org/JPCC

Investigation on the π-Dimer/σ-Dimer of 1,8-Dihydroxy-9,10-anthracenedione in the Process of Electrochemical Reduction by Using IR Spectroelectrochemical Cyclic Voltabsorptometry and Derivative Cyclic Voltabsorptometry

Wang-Xing Cheng,[†,‡] Bao-Kang Jin,*[,†] Peng Huang,[†,‡] Long-jiu Cheng,[†] Sheng-Yi Zhang,[†] and Yu-Peng Tian[†]

[†]Department of Chemistry, Anhui University, Hefei, Anhui 230039, People's Republic of China

[‡]Anhui University of Traditional Chinese Medicine, Hefei, Anhui 230038, People's Republic of China

Supporting Information

ABSTRACT: The electrochemical reduction of 1,8-dihydroxy-9,10-anthracenedione (Q) has been investigated by cyclic voltammetry (CV). Both 9,10-anthroquinone (AQ) and 1,8-methoxy-9,10-anthracenedione (DMeAQ) are reduced in two steps. First, they are reduced to the anion radical. Next, the anion radicals are reduced to the dianion. However, the CV of Q shows more cathodic and anodic peaks, which suggests the formation of a neutral- anion radical complex. To study the reaction mechanism of Q, in situ infrared (IR) spectroelectrochemistry, IR cyclic voltabsorptometry (CVA), and derivative cyclic voltabsorptometry (DCVA) spectroelectrochemical techniques are used to track the electrochemical reduction process. It is found that Q is reduced to $Q^{\bullet-}$, then $Q^{\bullet-}$ reacts with Q to produce dimer $Q_2^{\bullet-}$. What's more, both the π-dimer and σ-dimer can be observed during the electrochemical process by an IR spectroelectrochemical technique. As a result, a new reaction mechanism of Q has been proposed by this powerful approach.

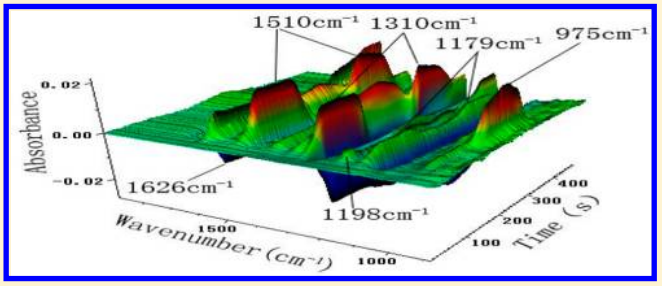

1. INTRODUCTION

An understanding of how electron transfer, proton transfer, and hydrogen bonding work together in organic redox couples to develop a detailed mechanism is a very important current goal in organic electrochemistry. They are well-represented in biological electron transport processes, playing key roles, for example, in the photosynthetic reaction center and in mitochondrial ATP synthesis.[1] Man has also found a number of uses for quinones, such as dyes[2] and as oxidizing and reducing agents in industrial[3] and laboratory scale chemical synthesis. In addition, a number of quinones have also been found to have medicinal properties, including antibiotic, antimicrobial, and anticancer activity.[4,5] Quinone compounds are widely distributed chemical groups in nature which play several different roles in living organisms,[6−11] and hydroxyquinones are of significant interest owing to their important biological functions.

The electrochemical reduction of hydroxyquinones has been studied widely.[12−20] The results show that the initially formed anion radical is protonated by the neutral quinone, and stabilization of reduced forms of the hydroxyquinones occurs by intramolecular hydrogen bonding between the hydroxylic proton and quinoidal oxygen. The formation of a neutral-anion radical complex has been proposed,[21,22] which has shown that some hydroxyquinones could undergo dimerization to form either σ- or π-dimers. For the formation of anion radical dimers, its has been proposed that formation of a π-dimer intermediate occurs before collapse of the two radical anions into a σ-bonded species for the case of delocalized π systems such as 9-cyanoanthracene.[23,24] In fact, the conclusive evidence for the formation of a π-dimer intermediate prior to formation of the σ-dimer has been provided.[25]

Recently, Macias and Evans have investigated the electrochemical reaction of several hydroxyquiones.[21] Two reduced steps, first to an anion radical and then to the dianion at more negative potentials, were observed. Cyclic voltammetry (CV) digital simulations were carried out to confirm the electrochemical reaction. The electrochemical process for 1,8-dihydroxy-9,10-anthraquione in acetonitrile has been suggested by reactions as follows

$$HQ + e = HQ^{\bullet-} \quad (1)$$

$$HQ^{\bullet-} + e = HQ^{2-} \quad (2)$$

$$2HQ^{\bullet-} = HQ + HQ^{2-} \quad (3)$$

Received: September 2, 2012
Revised: February 6, 2013
Published: February 7, 2013

$$HQ^{\bullet -} + HQ = (HQ)_2^{\bullet -} \quad (4)$$

Dimerization is one of the important organic radical reactions, and it has received great attention recently.[25−31] Dimers are commonly held together by covalent or hydrogen bonds. They are often important in the fields of biochemistry, especially medicine, where they are involved in the diagnosis of certain diseases. Usually, a π-dimer forming reaction is very rapid with the kinetics constant and relatively small equilibrium constant. However, a σ-dimer forming reaction has a slow rate and large equilibrium constant. Hence, to explore the conversion of π-dimer to σ-dimer with a CV experiment, a slow potential scan rate (long time window) should be carried out.

In this paper, the electrochemical reduction process of 9,10-anthroquinone (AQ), 1,8-dihydroxy-9,10-anthracenedione (Q), and 1,8-methoxy-9,10-anthracenedione (DMeAQ) was investigated under a lower potential scan rate. CV results show that two well-defined CV peaks are observed for AQ and DMeAQ, corresponding to AQ(DMeAQ)/AQ(DMeAQ)$^{\bullet -}$ and AQ-(DMeAQ)$^{\bullet -}$/AQ(DMeAQ)$^{2-}$; however, more than two sets of cathodic and anodic peaks are found for Q, which imply that the complex electrode reaction exists. Infrared (IR) cyclic voltabsorptometry (CVA) and derivative cyclic voltabsorptometry (DCVA) spectroelectrochemical techniques were used to study the electrochemical reduction of the three quinones. The obtained IR CVA and DCVA correspond to the various wavenumbers involved in the electrode process, which give more detailed information than the common CV.[32−37]

IR CVA results show that IR absorption peaks obtained from AQ, Q, and DMeAQ can be employed to track the electrochemical reaction and explore the electrode reaction. Absorbance of Q at 1518 and 1310 cm^{-1} corresponds to the reduction from Q to intermediate Q$^{\bullet -}$, and Q$^{\bullet -}$ was further reduced to dimer Q−Q$^{\bullet -}$, π-Q_2^{2-}, σ-Q_2^{2-}. The superimposed peak at 1310 cm^{-1} observed in a consecutive CV scan can be assigned to the σ-Q_2^{2-} dimer. A value of 1198 cm^{-1} is assigned to both Q$^{\bullet -}$ and Q−Q$^{\bullet -}$, and 1179 cm^{-1} is assigned to dimer Q−Q$^{\bullet -}$, π-Q_2^{2-}, σ-Q_2^{2-}, and σ-Q_2^{3-}. The absorbance at 972 cm^{-1} is assigned to υ_{C-O} of σ-Q_2^{3-} and σ-Q_2^{4-} and at 1626 cm^{-1} to $\upsilon_{C=O}$ of Q, Q$^{\bullet -}$, π-Q_2^{2-}, σ-Q_2^{2-}, and σ-Q_2^{3-}. So, a new electrochemical reaction mechanism of Q has been proposed by this powerful approach.

2. EXPERIMENTAL SECTION

2.1. Chemicals. 9,10-Anthroquinone (AQ, 98%), 1,8-dihydroxy-9,10-anthracenedione (Q, 97.5%), and anhydrous acetonitrile (AN, 99.8%) were used as received from Sigma-Aldrich. DMeAQ was synthesized as documented[35] and characterized by IR and ^{1}H NMR. Bu_4NClO_4 was prepared by a standard method,[38] recrystallized from ethanol, and dried overnight under reduced pressure at 100 °C before use and stored under vacuum. Before dissolving AQ, Q, and DMeAQ, blank solutions were bubbled with high purity nitrogen to remove oxygen. The AQ, Q, and DMeAQ solution was degassed with high purity nitrogen prior to the experiment and kept under nitrogen during measurements.

2.2. Voltammetry. Cyclic voltammetry (CV) experiments were conducted with an electrochemical analyzer CHI630C potentiostat. Working electrodes were 4 mm diameter planar Pt disks, a Pt wire auxiliary electrode, and Ag/AgCl reference electrode. The Pt disk working electrode was polished before each experiment with 0.05 μm α-alumina slurry, rinsed thoroughly with double distilled water, and sonicated in a nitric acid solution ($VHNO_3$:VH_2O = 1:1), acetone, alcohol, and acetonitrile solutions successively. All potentials are reported vs ferrocene, so the potential of the Pt disk working electrode was frequently measured in the ferrocenium (Fc^+)/ferrocene (Fc) solution and used to modify the potential in the experiment solution.

2.3. In Situ FT-IR Spectroelectrochemistry. FT-IR spectroscopic measurements were performed by an in situ method on a Nicolet Nexus 870 spectrometer equipped with a specular reflectance accessory (SMART iTR) and a HgCdTe/A(MCT/A) detector cooled with liquid nitrogen. All the experiments were carried out in a homemade reflection−absorption spectroelectrochemical cell. For rapid-scan time-resolved spectroscopic measurements, 25−60 interferograms were added to each spectrum; the sampling interval is 0.7−1.8 s; and the spectral resolution is 16 cm^{-1}. Experiment results were dealt with Grams/3D software. The resulting spectra were given as

$$A = \lg \frac{1}{T} = \lg \frac{R(E_R)}{R(E_S)}$$

where A and T represent absorbance and transmittance, respectively. E_S and E_R represent sampling potential and reference potential, and $R(E_S)$ and $R(E_R)$ represent single beam spectra obtained at E_R and E_S, respectively. By subtracting the reflection spectrum at the sampling potential E_S, $R(E_S)$, from the reflection spectrum at the reference potential E_R, $R(E_R)$, the background due to the absorption of the solvent system is eliminated. As a result, a negative-going sign of band and a positive-going sign of band indicate the increase and the decrease in absorption intensities of the bands at E_S, respectively.

2.4. Characterization of the Electrolysis Products. To confirm the dimer of $Q_2^{\bullet -}$, the electrolysis of Q has been done in a H-shaped electrolytic cell. The electrolytic product was characterized by microscope, IR, MS, and NMR in this work (Supporting Information).

3. RESULTS AND DISCUSSION

3.1. Electrochemical Study of AQ and DMeAQ. In aprotic solvents, quinones are known to undergo two successive one-electron reductions, accordingly forming a radical anion intermediate in the first step and the dianion in the second step.

Figure 1 shows the typical voltammetric signal of AQ in a thin-layer cell. As a general result, the AQ presents a voltammogram consisting of two couples of cathodic and anodic peaks. In the first step, one-electron reduction forms the anion radical and the dianiom sequentially. DMeAQ from methylated Q also has two cathodic and anodic peaks. It is very clear that DMeAQ has undergone one-electron reductions, forming sequentially the anion radical and dianiom. The CV of AQ and DMeAQ is almost the same as what has been reported.[20,21] The large peak−peak separation of the second reduction process of DMeAQ is due to the slow electron transfer rate in the quasi-reversible process.[39] Compared with the two half potentials ($E_{1/2}$) of AQ ($E^1_{1/2}$ = −1.26 V and $E^2_{1/2}$ = −1.65 V for the first and second electron-transfer step), $E_{1/2}$ of DMeAQ ($E^1_{1/2}$ = −1.44 V and $E^2_{1/2}$ = −1.69 V) shifts negatively, which is caused by the electron-donating effect of methoxy.

dx.doi.org/10.1021/jp3116947 | J. Phys. Chem. C 2013, 117, 3940−3948

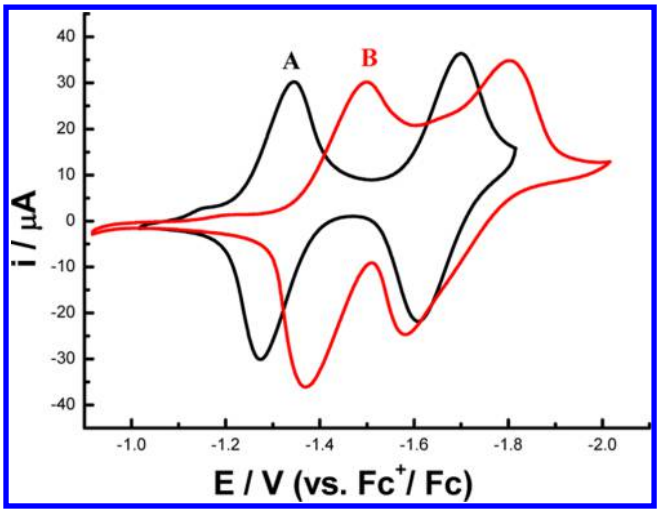

Figure 1. Thin-layer CV in AN solution with 0.2 M TBAP in a thin-layer cell of 10 mM AQ (A) and DMeAQ (B).

3.2. In-Situ FT-IR Spectroelectrochemistry of AQ and DMeAQ. The rapid-scan IR spectra recorded in situ during the CV scan of AQ in the 1000−1800 cm^{-1} region are shown in Figure 2A. The 3D spectra was gathered during the scan between −0.9 and −1.9 V. The spectrum recorded at −0.9 V was used as the reference spectrum. Three types of IR peaks are observed. The first type, including three distinct upward peaks at 1487, 1403, and 1243 cm^{-1}, is assigned to $\upsilon_{C=C}$ and υ_{C-O} of the semiquinone anion radical. The second is three distinct upward peaks at 1356, 1164, and 1056 cm^{-1}, which are assigned to υ_{C-O} of the final reduced product (dianion). The third, two downward peaks, at 1672 and 1102 cm^{-1}, is assigned to $\upsilon_{C=O}$ of quinone and $\upsilon_{Cl=O}$ of ClO_4^- (Figure 2A). The eight IR absorption peaks can be employed to track the corresponding species concentration during the electrochemical reaction. The peak at 1672 cm^{-1} is employed to track directly the disappearance of original reactant AQ, and 1356, 1164, and 1056 cm^{-1} are used to follow the formation of the dianion (AQ^{2-}); 1487, 1403, and 1243 cm^{-1} yielded information about intermediate $AQ^{\bullet-}$. The band at 1102 cm^{-1}, assigned to $\upsilon_{Cl=O,}$ represents the change of ClO_4^{-1} during the redox process.

The IR CVA of AQ (corresponding to Figure 2A) is shown in Figure 3A. There is a periodic increase and decrease of absorbance at 1487, 1403, and 1243 cm^{-1} with the sweep potential (time), corresponding to the reduction from AQ to

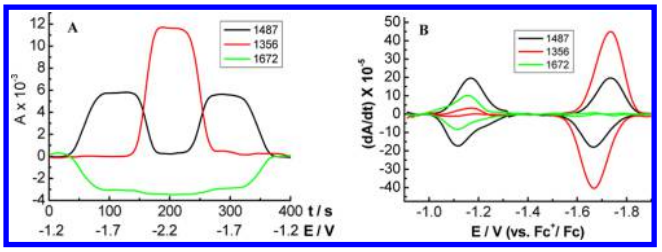

Figure 3. CVA (A) and selected DCVA (B) (smoothing with a fast Fourier transform smoothing algorithm) for the AQ electrochemical reaction at 1672, 1487, and 1356 cm^{-1}. To make the DCVA data readily comparable to CV, the DCVA data of 1672 cm^{-1} were multiplied by −1, and 1487 and 1356 cm^{-1} in the second reduction and the first oxidation were multiplied by −1.

intermediate $AQ^{\bullet-}$, and $AQ^{\bullet-}$ is further reduced to AQ^{2-}. Absorbance at 1356, 1164, and 1056 cm^{-1} (assigned to υ_{C-O} with the formation of the benzene ring skeleton vibration) gradually increases in the reduction process and reaches its maximum at nearly −1.9 V (200 s), and this absorbance diminishes during the oxidation process and then vanishes at −1.55 V (270 s). The absorbance at 1672 cm^{-1} gradually decreases in the reduction process and reaches minimum at nearly −1.9 V (200 s), and then the absorbance begins to increase at nearly −1.55 V (270 s) in the oxidation process and vanishes at −1.1 V (360 s).

It is apparent from Figure 3B that the shape of DCVA at 1487 cm^{-1} corresponding to intermediate $AQ^{\bullet-}$ is similar to that of CV shown in Figure 1A, where two redox couples are observed. Morphological DCVA couples of the absorbance at 1672 cm^{-1} correspond to the redox couple of $AQ/AQ^{\bullet-}$ (the first electrochemical step). The absorbance at 1356 cm^{-1} corresponds to the couple of $AQ^{\bullet-}/AQ^{2-}$ (the second electrochemical step). Both of them are the same as the corresponding CV shown in Figure 1A.

Figure 2B shows the rapid-scan IR spectra recorded in situ during the electrochemical process of DMeAQ in the 1000−1800 cm^{-1} region. The 3D spectra were gathered during the scan between −0.9 and −2.0 V. The spectrum recorded at −0.9 V was used as the reference spectrum. Two distinct upward peaks at 1526 and 1487 cm^{-1} are assigned to $\upsilon_{C=C}$ of the semiquinone anion radical, and two distinct upward peaks at 1356 and 1048 cm^{-1} are assigned to υ_{C-O} of final reduced production (dianion). One downward peak, at 1680 cm^{-1}, is assigned to $\upsilon_{C=O}$ of DMeAQ. The five IR absorption peaks can

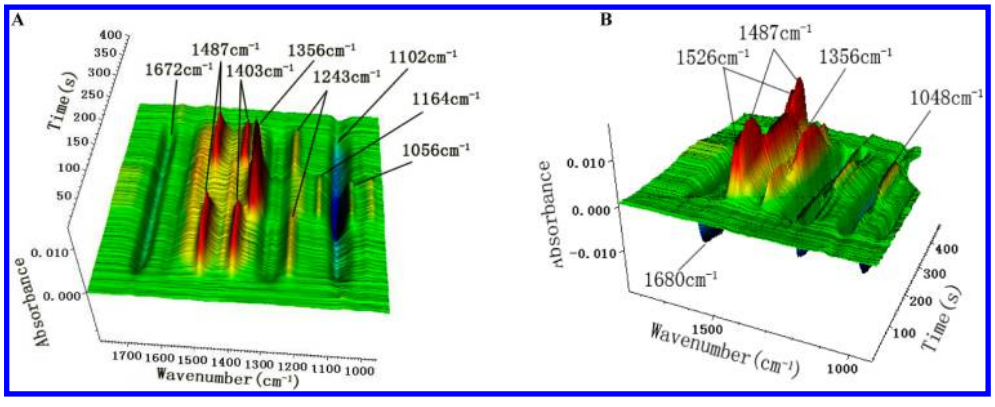

Figure 2. 3D spectra of in situ FT-IR spectroelectrochemistry corresponding to the thin-layer CV (Figure 1) of 5 mM AQ (A) and 10 mM DMeAQ (B) in AN solution with 0.2 M TBAP in the thin-layer cell, with potential scan rate 5 mV/s.

dx.doi.org/10.1021/jp3116947 | J. Phys. Chem. C 2013, 117, 3940−3948

be employed to track the electrochemical reaction. The peak at 1680 cm^{-1} can be employed to track directly the disappearance of the original reactant DMeAQ, and 1356 and 1048 cm^{-1} are used to follow the formation of product $DMeAQ^{2-}$. Peaks 1526 and 1487 cm^{-1} yield information about intermediate $DMeAQ^{\bullet-}$.

The IR CVA of DMeAQ (corresponding to Figure 1B) is shown in Figure 4A. There is a periodic increase and decrease

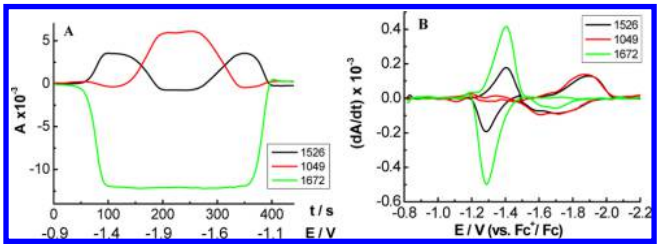

Figure 4. CVA (A) and DCVA (B) (smoothing with a fast Fourier transform smoothing algorithm) for the DMeAQ electrochemical reaction at 1526, 1049, and 1672 cm^{-1}. To make the DCVA data readily comparable to CV, the DCVA data of 1672 cm^{-1} were multiplied by −1, and 1526 and 1049 cm^{-1} in the second reduction and the first oxidation were multiplied by −1.

of absorbance at 1526 and 1487 cm^{-1} with the sweep potential (time), corresponding to the reduction from DMeAQ to intermediate $DMeAQ^{\bullet-}$, and $DMeAQ^{\bullet-}$ is further reduced to $DMeAQ^{2-}$. The absorbance at 1049 cm^{-1} (assigned to υ_{C-O} with the formation of the benzene ring skeleton vibration) gradually increases in the reduction process and reaches its maximum at nearly −2.0 V (220 s). This absorbance diminishes during the oxidation process and then vanishes at −1.1 V (400 s). Also, the absorbance at 1672 cm^{-1} gradually decreases in the reduction process and reaches minimum at nearly −1.4 V (100 s). The absorbance begins to increase at nearly −1.3 V (360 s) in the oxidation process.

It is also apparent from Figure 4B that the shape of DCVA at 1526 and 1487 cm^{-1} corresponding to intermediate $AQ^{\bullet-}$ is similar to that of CV shown in Figure 1B, where two redox couples are observed. Similarly, morphological DCVA couples at 1672 cm^{-1} correspond to the redox couple of DMeAQ/$DMeAQ^{\bullet-}$ in the first electrochemical step. The absorbance at 1049 cm^{-1} corresponds to the couple of $DMeAQ^{2-}$ in the second electrochemical reduced wave. The morphological DCVA couples are the same with the corresponding CV shown in Figure 1B.

On the basis of the results of CV and IR spectroelectrochemistry, we can confirm that a simple stepwise reduction can be used to express the electrochemical reaction of AQ and DMeAQ

$$AQ + e \rightleftharpoons AQ^{\bullet-} \quad (5)$$

$$AQ^{\bullet-} + e \rightleftharpoons AQ^{2-} \quad (6)$$

$$2AQ^{\bullet-} \rightleftharpoons AQ + AQ^{2-} \quad (7)$$

3.3. Electrochemical Study of Q. The typical CV for Q in a thin-layer cell under a slow potential scan wave is shown in Figure 5. It is surprising that four cathodic peaks (I_c–IV_c) and three anodic peaks (IV_a–II_a) can be observed under experimental conditions. This electrochemical behavior is extremely different from AQ and DMeAQ. Recently, Macias-Ruvalcaba and Evans[21] have investigated the electrochemical

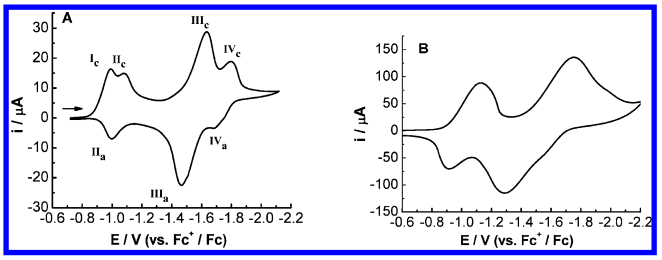

Figure 5. Thin-layer CV in AN solution with 0.2 M TBAP in the thin-layer cell of 10 mM Q with potential scan rate: (A) ν = 5 mV/s and (B) ν = 50 mV/s.

reduction of several hydroxyquiones. Two coupled CV peaks are found in the curves of the experiment. The forming of a neutral–anion radical complex, $HQ^{\bullet-} + HQ = HQ_2^{\bullet-}$, was suggested in their research. The result of digital simulation supports the existence of $HQ_2^{\bullet-}$ during the CV scan. It is obvious that our CV curve is greatly different from theirs.

It should be stated that our CV and in situ IR experiment were conducted in the thin-layer cell, with slow potential scan rate, type 5 mV/s. Hence, quinones can be electrolyzed completely, and the diffusion of species can be neglected. In addition, the potential scan rate is only 5 mV/s, which is much slower than what has been reported (3000 mV/s). However, the CV of Q with the high scan rate (ν = 50 mV/s) is similar to that of AQ and DMeAQ (Figure 5B). There are two coupled CV peaks in the curves of the experiments. Why are four cathodic peaks (I_c–IV_c) and three anodic peaks (IV_a–II_a) observed in the thin-layer cell under a low potential scan rate? A reasonable hypothesis is that slow chemical reactions coupled with the electron transfer occur in the thin-layer cell. As pointed out by Macias-Ruvalcaba, a neutral–anion radical complex formed during the electrochemical reduction of Q. One may ask that the dimer can be reduced further, or it can be changed into another form? To investigate the electrochemical reduction of Q in more detail, IR spectroelectrochemistry was utilized again.

3.4. In Situ FT-IR Spectroelectrochemistry of Q. The rapid-scan IR spectra recorded in situ during the electrochemical process of Q in the 1000–1800 cm^{-1} region are shown in Figure 6A. The 3D spectra were gathered during the scan between −0.7 and −2.1 V.

The IR peaks at 1310 cm^{-1} which increase and decrease with the sweep potential (time) are observed in Figure 6B. The similar change of IR peaks for AQ at 1478 and 1403 cm^{-1} and for DMeAQ at 1526, 1487, and 1356 cm^{-1} were discussed

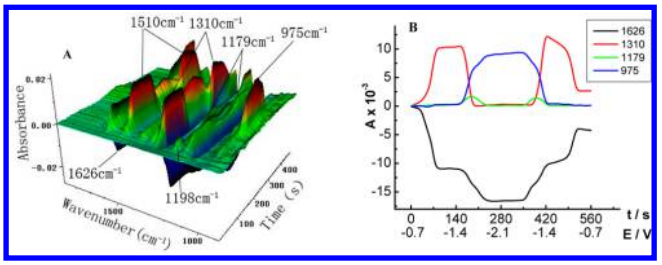

Figure 6. 3D spectra (A) of in situ FT-IR spectroelectrochemistry corresponding to the thin-layer CV of Figure 5A of 10 mM Q in AN solution with 0.2 M TBAP in a thin-layer cell, with potential scan rate 5 mV/s. CVA (B) (smoothing with a fast Fourier transform smoothing algorithm) for the Q electrochemical reaction at 1626, 1310, 1179, and 975 cm^{-1}.

dx.doi.org/10.1021/jp3116947 | J. Phys. Chem. C 2013, 117, 3940–3948

above. The IR peaks are assigned to $\upsilon_{C=C}$ and υ_{C-O} of the anion radical. However, two other types of IR absorption, peaks at 1198 and 1179 cm^{-1}, show different characters. It is clear that the IR peak at 1179 cm^{-1} can be observed only at 170−230 s (−1.55 ∼ −1.85 V) and 370−420 s (−1.85 ∼ −1.55 V). The potential is corresponding to peak III and IV on the CV curves (Figure 5A). The character of the IR peak, with its absorption increasing and decreasing during both the oxidization and reduction process, suggests that the IR peak at 1179 cm^{-1} should be assigned to an unknown intermediate. The IR absorption at 1198 cm^{-1} is more complex, which we will discuss later.

The IR CVA of Q (corresponding to Figure 6A) are shown in Figure 6B. A periodic increase and decrease of absorbance at 1310 and 1179 cm^{-1} changes with the sweep potential (time). It corresponded to the reduction from Q to intermediate $Q^{\bullet-}$, and $Q^{\bullet-}$ is further reduced to Q^{2-}. The absorbance at 975 cm^{-1} (assigned to υ_{C-O} of final reduced product Q^{2-}) gradually increases in the reduction process and reaches its first equilibrium at nearly −1.7 V (195 s), whose process can be assigned to the reduction from $Q^{\bullet-}$ to Q^{2-}. Then, the absorbance reaches its maximum at nearly −1.9 V (235 s), which means the final reduced product is being formed. These results imply that some complex reactions exist in the process of the reduction from $Q^{\bullet-}$ to Q^{2-}. The absorbance at 975 cm^{-1} diminishes during the oxidation process and then vanishes at −1.4 V (425 s). Also the absorbance at 1626 cm^{-1} gradually decreases in the reduction process and reaches its first equilibrium at nearly −1.15 V (85 s), which corresponded to the reduction process from Q to intermediate $Q^{\bullet-}$. The absorbance at 1626 cm^{-1} reaches its minimum at nearly −1.9 V (240 s), whose process can be assigned to the reduction from $Q^{\bullet-}$ to Q^{2-}.

Interestingly, the IR absorbance at 1626 and 1310 cm^{-1} does not return to baseline after one potential cycle. The absorbance begins to increase at nearly −1.8 V (350 s) in the oxidation process and reaches a steady state value. The results coming from CV and IR CVA both strongly suggest that an irreversible electrochemical/chemical process exists in the electrochemical reaction of Q.

3.5. Electrochemical Reaction Mechanism of Q. Evans etc.[21,22] reported that the dimers were formed in the electrochemical reduction of hydroxyquinones. A more complex reaction mechanism was being shown as reactions 1−4, and the guess was supported by the result of digital simulation under the condition of semi-infinite diffusion and of relative high potential scan rate (0.1−3 V/s). However, the electrochemical route can not explain our experimental results. To investigate the electrochemical nature of Q, CV curves under consecutive scan were recorded, and the results are shown in Figure 7A.

The peak currents of I_c and II_c are the largest in the first scan, which decrease rapidly in the second and third scans. The oxidation peak corresponding to I_c is not observed in the CV curves in the potential range. The peak current of II_a is much smaller than that of II_c. The results indicate that the redox process of I_c, II_c, and IIa is irreversible. The I_c and II_c are assigned to the reduction from Q to $Q^{\bullet-}$. The III_c and IV_c are assigned to the reduction of $Q^{\bullet-}$ and Q^{2-}. The IVc shows some irreversibility characteristics.

IR CVA results obtained from Q provide more information, which can be employed to track the electrochemical reaction and explore the electrode reaction.

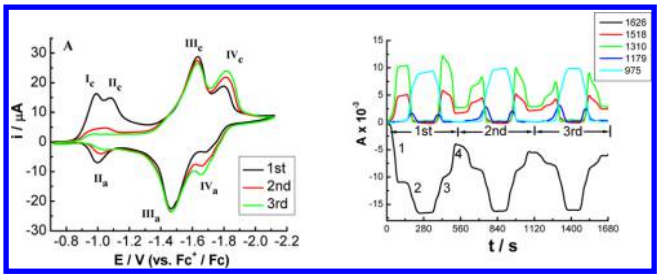

Figure 7. Continuous CV in AN solution with 0.2 M TBAP in a thin-layer cell of 10 mM Q (A) and corresponding CVA (B) of in situ FT-IR spectroelectrochemistry, with potential scan rate 5 mV/s.

The absorbance at 1626 cm^{-1}, assigned to $\upsilon_{C=O}$ of Q, shows four distinct steps. Steps 1 and 2 stand for the reduced process and steps 3 and 4 for the oxidized process during the CV scan. Step 1 is corresponding to the reduction from Q to $Q^{\bullet-}$, and step 2 is corresponding to the reduction from $Q^{\bullet-}$ to Q^{2-}. In the oxidation process, steps 3 and 4 are corresponding to Q^{2-}/$Q^{\bullet-}$ and $Q^{\bullet-}$/Q, respectively. However, after the first potential scan, the IR absorption does not return to the base value. In addition, the absorption at step 1 decreased rapidly with the number of the cycles increasing. In fact, step 1 disappears completely in the fifth scan (not shown in Figure 7B). This result is consistent with the CV curves (Figure 7A). It strongly suggests that the irreversible electrochemical/chemical process occurs under experimental conditions. Accordingly, new species exist after the first CV scan.

The absorbance at 1310 cm^{-1}, assigned to υ_{C-O} of $Q^{\bullet-}$ and $Q_2^{\bullet-}$, shows a similar character. That the absorption cannot return to baseline also implies that a new species was produced after the first CV scan. Interestingly, a superimposed absorption peak at 1310 cm^{-1} is observed in the second and third scans. The absorption of the superimposed peak increases with the number of the potential cycles increasing. Finally, only the superimposed peak can be observed after several times of CV scan.

The absorbance at 1179 cm^{-1} increases and decreases periodically with the sweep potential (time) in one CV scan. The absorption gradually increases with the absorption at 1310 cm^{-1} decreasing. It reaches its maximum at nearly −1.4 V (180 s) and then gradually decreases and finally vanishes in the reduction process. Meanwhile, we find that the absorption at 975 cm^{-1} appears before the absorption at 1179 cm^{-1} reaches its maximum value. The absorption at 975 cm^{-1} reaches its maximum value, while the absorption at 1179 cm^{-1} vanishes completely. The absorbance repeats this process in the oxidation process. These results mean that the absorbance at 1179 cm^{-1} can be assigned to an unknown intermediate which is generated from $Q^{\bullet-}$ and then changed to Q^{2-}.

On the basis of the discussion above, we can propose the electrochemical reduction mechanism of Q as follows

$$Q + e \rightleftharpoons Q^{\bullet-} \quad (8)$$

$$Q^{\bullet-} + Q \rightleftharpoons Q_2^{\bullet-} \quad (9)$$

$$Q_2^{\bullet-} + e \rightleftharpoons Q_2^{2-} \quad (10)$$

$$Q_2^{2-} + e \rightleftharpoons Q_2^{3-} \quad (11)$$

$$Q_2^{3-} + e \rightleftharpoons Q_2^{4-} \quad (12)$$

dx.doi.org/10.1021/jp3116947 | J. Phys. Chem. C 2013, 117, 3940−3948

The dimerzations are extensively observed in the reduction of quinone. As we know, two kinds of dimer were proposed: π-dimer and σ-dimer. Now we want to explore which kind of dimer exists in the electrochemical reduction of Q.

On the basis of the chemical structure of Q, the anion radicals can react with a neutral molecule to form a π-dimer, in which the two π systems interact in a face-to-face manner. An extra interaction force comes from intermolecular H-bonding. The π-dimerization reactions show rather small equilibrium constant and large rate constants. To explore the nature of the dimers, we reconsider Figure 7 again. As we discussed above, the current peaks I_c and II_c are assigned to the electrochemical reduction from Q to $Q^{\bullet-}$ and $Q_2^{\bullet-}$ to Q_2^{2-}, respectively. The peak II_a, corresponding to II_c, is reoxidized from Q_2^{2-} to $Q_2^{\bullet-}$. In consecutive CV scan experiments, Q diminishes gradually, and only $Q_2^{\bullet-}$ exists at last. Hence, the peak current of II_c and II_a should increase gradually and finally reach a steady state, while the peak of I_c decreases gradually and disappears finally. Although the peak I_c decreases with increasing scan times as we expected, the peaks of II_a and II_c also decrease with increasing scan times. It implies that $Q_2^{\bullet-}$ is not stable in the experimental time and that more complex electrochemical processes exist.

The changes of absorbance at 1310 cm^{-1} in consecutive CV scan experiments (Figure 8A) can be used to explain the

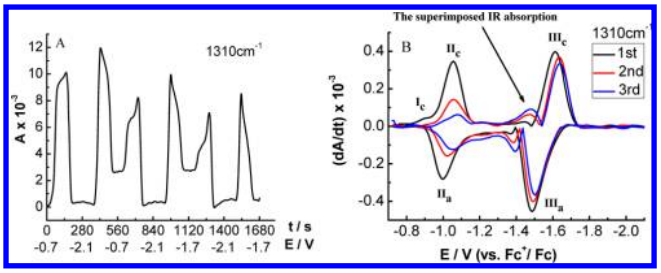

Figure 8. CVA (A) and DCVA of 1310 cm^{-1} (B) corresponding to Figure 7A. To make the DCVA data readily comparable to CV, the III_c reduction and III_a oxidation in the DCVA data were multiplied by −1.

complex electrochemical reduction reaction. The absorption gradually increases at first in the first CV scan for the electrochemical reduction from Q to $Q^{\bullet-}$ which forms $Q_2^{\bullet-}$ sequentially. The superimposed absorption peaks are clearly observed at −1.52 V in the reduction process and at −1.42 V in the oxidization process in the second and third scans. The redox peaks show that the reaction of π-$Q_2^{\bullet-}$(π-Q_2^{2-}) irreversibly forming σ-$Q_2^{\bullet-}$(σ-Q_2^{2-}) is slow, and the absorption increases with the number of potential cycles increasing because of the concentration of σ-$Q_2^{\bullet-}$(σ-Q_2^{2-}) increasing with time. At the same time, the σ-$Q_2^{\bullet-}$ can also be reduced to σ-Q_2^{2-} in the second and third CV scans for the reason that a new couple of cathodic and anodic peaks corresponding to the superimposed absorption peak appeared in the DCVA (Figure 8B). The peak current increased with the number of the potential cycle increasing. So these reactions should be added to the mechanism as follows

$$Q + e \rightleftharpoons Q^{\bullet-} \tag{13}$$

Quick reaction:

$$Q + Q^{\bullet-} \rightarrow Q\text{–}Q^{\bullet-} \quad \text{or} \quad \pi\text{-}Q_2^{\bullet-} \tag{14}$$

$$Q^{\bullet-} \quad \text{or} \quad \pi\text{-}Q_2^{\bullet-} + e \rightleftharpoons \pi\text{-}Q_2^{2-} \tag{15}$$

Slow reaction:

$$\begin{cases} \pi\text{-}Q_2^{\bullet-} \rightarrow \sigma\text{-}Q_2^{\bullet-} \\ \pi\text{-}Q_2^{2-} \rightarrow \sigma\text{-}Q_2^{2-} \end{cases} \tag{16}$$

$$\sigma\text{-}Q_2^{\bullet-} + e \rightleftharpoons \sigma\text{-}Q_2^{2-} \tag{17}$$

To confirm the electrochemical process, CV scan experiments, one in small range potential and the other with more positive potential, were conducted. Figure 9A shows the CV of

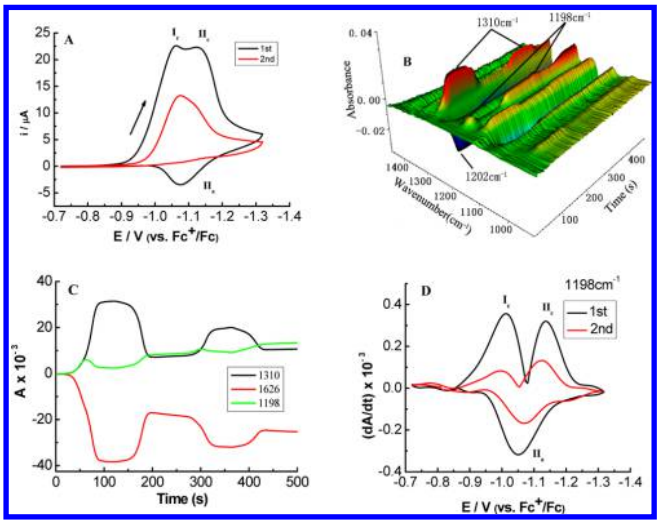

Figure 9. CV (A), corresponding 3D spectra (B) of in situ FT-IR spectroelectrochemistry, CVA (C) and DCVA of 1198 cm^{-1} (D) in AN solution with 0.2 M TBAP in a thin-layer cell of 10 mM Q with potential scan rate 5 mV/s and potential range −0.7 ~ −1.3 V in a thin-layer cell. To make the DCVA data readily comparable to CV, the second reduction and the first oxidation in the DCVA data were multiplied by −1.

Q in the potential range of −0.7 ~ −1.3 V. Two cathodic peaks appear in the first scan CV. The first reduction peak is assigned to the reduction of Q to $Q^{\bullet-}$; the second is assigned to the reduction from $Q_2^{\bullet-}$ to Q_2^{2-}. Only one anodic peak, corresponding to the oxidation of Q_2^{2-} to $Q_2^{\bullet-}$, is observed. The height of the anodic peak is much smaller than that of the cathodic peak. The reason may be that Q is reduced to $Q^{\bullet-}$, which reacts with Q to form π-$Q_2^{\bullet-}$. Soon enough (reaction 14), π-$Q_2^{\bullet-}$ irreversibly changes to σ-$Q_2^{\bullet-}$ with slow rate constant (reaction 16). The irreversible reaction can be verified by the fact that no appearance of the anodic peak can be observed in the second CV.

The change of absorbance at 1310 cm^{-1} comes from the corresponding 3D spectra of in situ FT-IR spectroelectrochemistry (Figure 9B), and CVA (Figure 9C) also supports the electrode reaction described by reactions 13−17. The absorbance at 1310 cm^{-1} is assigned to $Q^{\bullet-}$, Q–$Q^{\bullet-}$, π-Q_2^{2-}, and σ-Q_2^{2-}. During the first cycle (0−240 s), the absorbance gradually increases in the reduction process and reaches its maximum at nearly −1.2 V (90 s), corresponding to the reduction from Q to $Q^{\bullet-}$ and to π-Q_2^{2-}. The absorbance diminishes during the oxidation process which corresponds to the oxidation from π-Q_2^{2-} to $Q_2^{\bullet-}$. Then the absorption "vanishes" at −1.0 V (190 s). Again the absorption does not come back to the baseline, implying that the reaction of the forming dimer is irreversible, which makes less Q exist in the

dx.doi.org/10.1021/jp3116947 | J. Phys. Chem. C 2013, 117, 3940−3948

thin-layer cell after a CV scan. As a result, the change of IR absorbance at 1310 cm^{-1} decreases rapidly at the second cycle (241−480 s).

Now, we focus our attention on the IR absorbance at 1198 cm^{-1}. In the potential range between −0.7 and −1.3 V (in the reduction process of 0 ∼ 120 s)—which corresponds to the reduction peaks of I_c and II_c—the absorption at 1198 cm^{-1} shows a "peak" shape curve, while the absorption at 1310 cm^{-1} shows an "S" shape curve. In the oxidation process, the IR absorbance at 1310 cm^{-1} at −1.2 to −1.0 V decreases, while the absorbance at 1198 cm^{-1} increases. The result indicates that the absorbance of 1310 and 1198 cm^{-1} comes from different species. One reasonable explanation is that the IR absorbance at 1198 cm^{-1} is from two kinds of dimers, both π-$Q_2^{\bullet-}$ and σ-$Q_2^{\bullet-}$.

Two reduction peaks (I_c and II_c) can be clearly observed in the DCVA (Figure 9D). The two peaks are corresponding to the reduction from Q to $Q^{\bullet-}$ and then to π-Q_2^{2-}. The peak current of I_c and II_c is smaller in the second CV cycle than that in the first CV cycle because the reduction forms a stable σ-dimer (σ-$Q_2^{\bullet-}$) which cannot be oxidized under experimental conditions. As a result, the stable IR absorbance at 1198 is observed after the CV scan.

Figure 10A shows the CV of Q in the potential range of 0.28 ∼ −1.32 V. It is obvious that a new oxidation wave (I_a) at +0.12

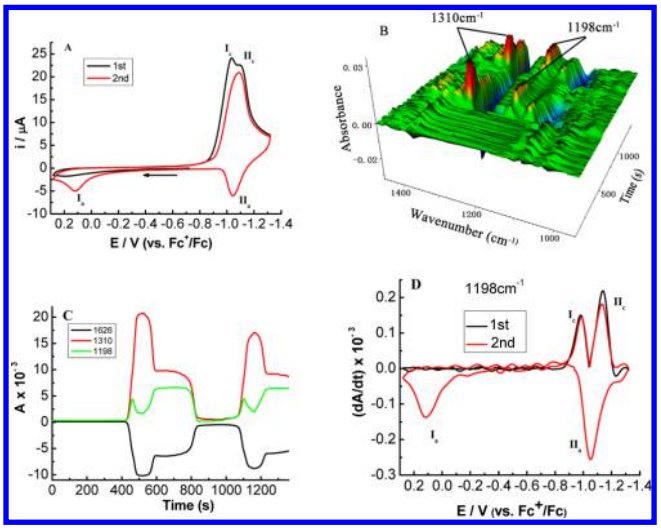

Figure 10. CV (A), correponding 3D spectra (B) of in situ FT-IR spectroelectrochemistry, CVA (C) and DCVA of 1198 cm^{-1} (D) in AN solution with 0.2 M TBAP in a thin-layer cell of 10 mM Q with potential scan rate 5 mV/s and potential range 0.28 ∼ −1.32 V in the thin-layer cell. To make the DCVA data readily comparable to CV, the second reduction and the first oxidation in the DCVA data were multiplied by −1.

V appears after a first reduction scan. There is no I_a in Figure 9A, which means that σ-$Q_2^{\bullet-}$ cannot be oxidized in the potential range of −0.7 ∼ −1.3 V. However, a new oxidization peak (I_a) appears at +0.12 V when the CV is scanned to a more positive potential. So the I_a can be assigned to the reaction that σ-$Q_2^{\bullet-}$ is electrochemically oxidized to Q.[20,25] The guess can be confirmed by IR experiments.

Corresponding 3D spectra of in situ FT-IR spectroelectrochemistry and CVA are shown in Figure 10B and 10C. Absorbance at 1310 cm^{-1} has the same change as Figure 10B and 10C at first. However, with scanning more positive potential at nearly +0.12 V (about 810 s), the absorbance decreases gradually again and almost comes to baseline, which strongly suggests that the oxidation from σ-$Q_2^{\bullet-}$ to Q occurs.

In the oxidation process (in the potential range between 0.28 ∼ −1.32 V), two oxidation peaks at −1.0 and +0.12 V are observed in CV. At E_{pa} = −1.0 V, the absorption of 1198 cm^{-1} appears again, indicating that π-Q_2^{2-} is electrochemically oxidized to π-$Q_2^{\bullet-}$ which is changed to form the σ-dimer (σ-$Q_2^{\bullet-}$) slowly. However, after E_{pa} = +0.12 V, the absorption of 1198 cm^{-1} decreases and finally comes back to baseline. At the same time, the absorption of 1626 cm^{-1} also comes back to baseline. All the results indicate that the σ-dimer is oxidized to Q, so Q has been recovered. Two reduction peaks (I_c and II_c) can be observed in the DCVA of 1198 cm^{-1} more clearly than that in the CV (Figure 10D). The peak current of I_c and II_c in the first CV is close to that in the second CV because the σ-dimer (σ-$Q_2^{\bullet-}$) is oxidized to Q under experimental conditions.

On the basis of the above discussion, the Q is reduced to Q^- (reaction 18) which reacts with Q and forms Q−$Q^{\bullet-}$ or π-$Q_2^{\bullet-}$ quickly (reaction 19). Q−$Q^{\bullet-}$ or π-$Q_2^{\bullet-}$ is reduced to π-Q_2^{2-} (reaction 20). At the same time, π-$Q_2^{\bullet-}$ and π-Q_2^{-} irreversibly change and form σ-$Q_2^{\bullet-}$ and σ-Q_2^{2-} slowly (reaction 21). The σ-$Q_2^{\bullet-}$ is reduced to σ-Q_2^{2-} (reaction 22) which is reduced to σ-$Q_2^{\bullet 3-}$ (reaction 23). σ-$Q_2^{\bullet 3-}$ is reduced to σ-Q_2^{4-} (reaction 24). The σ-$Q_2^{\bullet-}$ can be oxidized at +0.12 V (reaction 25). So the electrochemical reaction mechanism of Q was proposed as follows

$$Q + e \underset{}{\overset{E_{pc}=-0.97V}{\rightleftharpoons}} Q^{\bullet-} \tag{18}$$

Quick reaction:

$$Q + Q^{\bullet-} \rightarrow Q{-}Q^{\bullet-} \quad \text{or} \quad \pi\text{-}Q_2^{\bullet-} \tag{19}$$

$$Q{-}Q^{\bullet-} \quad \text{or} \quad \pi\text{-}Q_2^{\bullet-} + e \underset{E_{pc}=-1.01V}{\overset{E_{pa}=-1.04V}{\rightleftharpoons}} \pi\text{-}Q_2^{2-} \tag{20}$$

Slow reaction:

$$\begin{cases} \pi\text{-}Q_2^{\bullet-} \rightarrow \sigma\text{-}Q_2^{\bullet-} \\ \pi\text{-}Q_2^{2-} \rightarrow \sigma\text{-}Q_2^{2-} \end{cases} \tag{21}$$

$$\sigma\text{-}Q_2^{\bullet-} + e \underset{E_{pa}=-1.42V}{\overset{E_{pc}=-1.52V}{\rightleftharpoons}} \sigma\text{-}Q_2^{2-} \tag{22}$$

$$\sigma\text{-}Q_2^{2-} + e \underset{E_{pa}=-1.48V}{\overset{E_{pc}=-1.62V}{\rightleftharpoons}} \sigma\text{-}Q_2^{\bullet 3-} \tag{23}$$

$$\sigma\text{-}Q_2^{\bullet 3-} + e \underset{E_{pa}=-1.66V}{\overset{E_{pc}=-1.87V}{\rightleftharpoons}} \sigma\text{-}Q_2^{4-} \tag{24}$$

$$\sigma\text{-}Q_2^{\bullet-} - e \xrightarrow{E_{pa}=0.12V} 2Q \tag{25}$$

4. CONCLUSION

The electrochemical characteristics of AQ, Q, and DMeAQ were studied by CV and in situ IR spectroelectrochemistry in a thin-layer cell. The results show that AQ and DMeAQ can be explained by normal stepwise reduction to the anion radical and dianion. However, Q should be explained by the formation of dimer between neutral quinone and the anion radical, which can be comfirmed by IR CVA and DCVA as well as continuous

dx.doi.org/10.1021/jp3116947 | J. Phys. Chem. C 2013, 117, 3940−3948

CV and IR CVA. Our experimental results show that two types of dimer, π-dimer and σ-dimer, form in the electrochemical reaction. The reaction mechanism can be explained by the following sequences: Q is reduced to $Q^{\bullet-}$; $Q^{\bullet-}$ reacts with Q and forms π-$Q_2^{\bullet-}$ quickly; and π-$Q_2^{\bullet-}$ irreversibly changes and forms σ-$Q_2^{\bullet-}$ with slow rate constant. The detailed mechanism of electrochemical reduction of Q can be proposed as reactions 18−25.

■ ASSOCIATED CONTENT

Supporting Information

The electrolysis of Q was done in a H-shaped electrolytic cell, and the electrolytic product was characterized by microscope, IR, MS, and NMR. This material is available free of charge via the Internet at http://pubs.acs.org.

■ AUTHOR INFORMATION

Corresponding Author

*Phone and Fax: +86 551 5107342. E-mail: bkjinhf@yahoo.com.cn.

Notes

The authors declare no competing financial interest.

■ ACKNOWLEDGMENTS

Support by the National Nature Foundation of China (Grants 21175001, 21273008, and 21275006), the Program for New Century Excellent Talents in University (China NECT-07-0002), Doctoral Program Foundation of the Ministry of Education of China, the Foundation of Scientific Innovation Team of Anhui Province (2006KJ007TD), and the 211 Project of Anhui University is acknowledged.

■ REFERENCES

(1) Garrett, R. H.; Grisham, C. M. *Biochemistry*; Thomson Brooks/Cole: Belmont, CA, 2005.

(2) Hattori, M. In *Kirk-Othmer Encyclopedia of Chemical Technology*, 5th ed.; Seidel, A., Ed.; John Wiley & Sons: Hoboken, NJ, 2004; Vol. *9*, pp 300−349.

(3) A particularly significant industrial use of quinones is as the "hydrogen carrier" in the production of hydrogen peroxide: Eul, M.; Moeller, A.; Steiner, N. In *Kirk-Othmer Encyclopedia of Chemical Technology*, 5th ed.; Seidel, A., Ed.; John Wiley & Sons: Hoboken, NJ, 2004; Vol. *14*, pp 42−51.

(4) Quinones are most commonly used as mild oxidizing agents and as dehydrogenating reagents, particularly for aromatization: Finley, K. T. In *Kirk-Othmer Encyclopedia of Chemical Technology*, 5th ed.; Seidel, A., Ed.; John Wiley & Sons: Hoboken, NJ, 2004; Vol. *21*, pp 238−270.

(5) Bautista-Martinez, J. A.; Gonzalez, I.; Aguilar-Martinez, M. Correlation of Voltammetric Behavior of α-Hydroxy and α-Methoxy Quinones with the Change of Acidity Level in Acetonitrile. *J. Electroanal. Chem.* **2004**, *573*, 289−298.

(6) McNew, G. L. The Natural and Synthetic Quinones in Relation to the Functions of Plants. *Bull. Torrey Bot. Club* **1950**, *77*, 294−297.

(7) Monks, T. J.; Jones, D. C. The Metabolism and Toxicity of Quinones, Quinonimines, Quinone Methides, and Quinone-Thioethers. *Curr. Drug Metab.* **2002**, *3*, 425−438.

(8) Plyta, Z. F.; Li, T.; Papageorgiou, V. P.; Mellidis, A. S.; Assimopoulou, A. N.; Pitsinos, E. N.; Couladouros, E. A. Inhibition of Topoisomerase I by Naphthoquinone Derivatives. *Bioorg. Med. Chem. Lett.* **1998**, *8*, 3385−3390.

(9) Papageorgiou, V. P.; Assimopoulou, A. N.; Couladouros, E. A.; Hepworth, D.; Nicolaou, K. C. The Chemistry and Biology of Alkannin, Shikonin, and Related Naphthazarin Natural Products. *Angew. Chem., Int. Ed.* **1999**, *38*, 270−301.

(10) Grolig, J.; Wagner, R. *Ullmann's Encyclopedia of Industrial Chemistry*; Wiley-VCH Verlag GmbH & Co. KGaA: Germany, 2005, DOI: 10.1002/14356007.a17-067.

(11) Shi, M.; Gozal, E.; Choy, H. A.; Forman, H. J. Extracellular Glutathione and Gamma-Glutamyl Transpeptidase Prevent H_2O_2-Induced Injury by 2,3-Dimethoxy-1,4-naphthoquinone. *Free Radical Biol. Med.* **1993**, *15*, 57−67.

(12) Ferraz, P. A. L.; de Abreu, F. C.; Pinto, A. V.; Glezer, V.; Tonholo, J.; Goulart, M. O. F. Electrochemical Aspects of the Reduction of Biologically Active 2-Hydroxy-3-alkyl-1,4-naphthoquinones. *J. Electroanal. Chem.* **2001**, *507*, 275−286.

(13) Gomez, M.; Gonzalez, F. J.; Gonzales, I. Intra and Intermolecular Hydrogen Bonding Effects in the Electrochemical Reduction of α-Phenolic-naphthoquinones. *J. Electroanal. Chem.* **2005**, *578*, 193−202.

(14) Bautista-Martınez, J. A.; Frontana, C.; Solano-Peralta, A.; Reyes-Hernandez, C. I.; Cuevas, G.; Gonzalez, I.; Aguilar-Martınez, M. Influence of the Substituent on the Reactivity of Anilinoperezones. Analysis of the Influence of the C(12)-C(13) Double Bond. *ECS Trans.* **2007**, *3*, 45−54.

(15) Frontana, C.; Gonzalez, I. Structural Factors Affecting the Reactivity of the Natural a-Hydroxy Benzoquinones. An Electrochemical and ESR Study. *ECS Trans.* **2007**, *3*, 13−23.

(16) Frontana, C.; Gomez, M.; Gonzalez, I. Intra vs Intermolecular Association Processes in the Radical Anions of b-Hydroxyquinones. Influence on the Structural Properties of the Radical Anion of Julgone. *ECS Trans.* **2007**, *3*, 37−44.

(17) Shamsipur, M.; Siroueinejad, A.; Hemmateenejad, B.; Abbaspour, A.; Sharghi, H.; Alizadeh, K.; Arshadi, S. Cyclic Voltammetric, Computational, and Quantitative Structure−Electrochemistry Relationship Studies of the Reduction of Several 9,10-anthraquinone Derivatives. *J. Electroanal. Chem.* **2007**, *600*, 345−358.

(18) Hernandez-Munoz, L. S.; Gomez, M.; Gonzalez, F. J.; Gonzalez, I.; Frontana, C. Towards a Molecular-Level Understanding of the Reactivity Differences for Radical Anions of Juglone and Plumbagin: an Electrochemical and Spectroelectrochemical Approach. *Org. Biomol. Chem.* **2009**, *7*, 1896−1903.

(19) Gonzalez, I.; Frontana, C.; Gomez, M.; Aguilar, M.; Bautista, J. A.; Macıas, N. A.; Salas, M.; Astudillo, P. D.; Gonzalez, F. J. Modifying the Reactivity of the Reduced Intermediates of Quinones by Structural Changes and Intra and Intermolecular Hydrogen Bonding. *ECS Trans.* **2007**, *3*, 25−36.

(20) Macias-Ruvalcaba, N. A.; Felton, G. A. N.; Evans, D. H. Contrasting Behavior in the Reduction of 1,2-Acenaphthylenedione and 1,2-Aceanthrylenedione. Two Types of Reversible Dimerization of Anion Radicals. *J. Phys. Chem. C* **2009**, *113*, 338−345.

(21) Macias-Ruvalcaba, N. A.; Evans, D. H. Association Reactions of the Anion Radicals of Some Hydroxyquinones: Evidence for Formation of π- and σ-Dimers As Well As a Neutral−Anion Radical Complex. *J. Phys. Chem. C* **2010**, *114*, 1285−1292.

(22) Hammerich, O.; Parker, V. D. Are Low or Negative Activation Enthalpies Consistent with the Alleged One Step Mechanism for the Dimerization of 9-Substituted Anthracene Anion Radicals? *Acta Chem. Scand. Ser. B* **1983**, *37*, 379−392.

(23) Hammerich, O.; Parker, V. D. Ion Radical Cleavage Reactions. IV. The Effect of the Halogen in Determining the Mechanism of Cleavage of Halide Ion During the Reduction of 9-Cyano-10-haloanthracenes. *Acta Chem. Scand. Ser. B* **1983**, *37*, 851−856.

(24) Hammerich, O.; Parker, V. D. Molecular Structures of Gaseous (Monomethylamino) Dimethylborane, Bis(monomethylamino)-methylborane, and Tris(monomethylamino)borane, $(CH_3)(3\text{-}n)B(NHCH_3)(n)$, n = 1,2,3, Studied by Electron Diffraction. *Acta Chem. Scand. Ser. B* **1981**, *35*, 341−357.

(25) Gallardo, I.; Guirado, G.; Marquet, J.; Vilà, N. Evidence for a π Dimer in the Electrochemical Reduction of 1,3,5-Trinitrobenzene: A Reversible N_2-Fixation System. *Angew. Chem., Int. Ed.* **2007**, *46*, 1321−1325.

(26) Todres, Z. V. *Organic Ion Radicals. Chemistry and Applications*; Dekker: New York, 2003.

(27) Zimmer, J. P.; Richards, J. A.; Turner, J. C.; Evans, D. H. Electrochemical Reduction of α,β-Unsaturated Ketones. *Anal. Chem.* **1971**, *43*, 1000−1006.
(28) Kraiya, C.; Singh, P.; Todres, Z. V.; Evans, D. H. Voltammetric Studies of the Reduction of *cis*- and *trans*-α-Nitrostilbene. *J. Electroanal. Chem.* **2004**, *563*, 171−180.
(29) Yurchenko, O.; Freytag, D.; Borg, L.; Zentel, R.; Heinze, J.; Ludwigs, S. Electrochemically Induced Reversible and Irreversible Coupling of Triarylamines. *J. Phys. Chem. B* **2012**, *116*, 30−39.
(30) Nepomnyashchii, A. B.; BrÖring, M.; Ahrens, J.; Bard, A. J. Chemical and Electrochemical Dimerization of BODIPY Compounds: Electrogenerated Chemiluminescent Detection of Dimer Formation. *J. Am. Chem. Soc.* **2011**, *133*, 19498−19504.
(31) Macías-Ruvalcaba, N. A.; Telo, J. P.; Evans, D. H. Studies of the Electrochemical Reduction of Some Dinitroaromatics. *J. Electroanal. Chem.* **2007**, *600*, 294−302.
(32) Kuwana, T.; Dariington, R. K.; Leedy, D. W. Electrochemical Studies Using Conducting Glass Indicator Electrodes. *Anal. Chem.* **1964**, *36*, 2023−2025.
(33) Astuti, Y.; Topoglidis, E.; Briscoe, P. B.; Fantuzzi, A.; Gilardi, G.; Durrant, J. R. Proton-Coupled Electron Transfer of Flavodoxin Immobilized on Nanostructured Tin Dioxide Electrodes: Thermodynamics versus Kinetics Control of Protein Redox Function. *J. Am. Chem. Soc.* **2004**, *126*, 8001−8009.
(34) Astuti, Y.; Topoglidis, E.; Gilardi, G.; Durrant, J. R. Cyclic Voltammetry and Voltabsorptometry Studies of Redox Proteins Immobilised on Nanocrystalline Tin Dioxide Electrodes. *Bioelectrochemistry* **2004**, *63*, 55−59.
(35) Jin, B. K.; Li, L.; Huang, J. L.; Zhang, S. Y.; Tian, Y. P.; Yang, J. X. IR Spectroelectrochemical Cyclic Voltabsorptometry and Derivative Cyclic Voltabsorptometry. *Anal. Chem.* **2009**, *81*, 4476−4481.
(36) Shi, T. S.; Sun, H. R.; Cao, X. Z.; Tao, J. Z. Spectroelectrochemical Characteristics of Tetrakis(4-nitrophenyl) porphyrin Manganese Complex. *Chem. J. Chin. Univ.* **1994**, *15*, 966−969.
(37) Jin, B. K.; Liu, P.; Wang, Y.; Zhang, Z. P.; Tian, Y. P.; Yang, J. X.; Zhang, S. Y.; Cheng, F. L. Rapid-Scan Time-Resolved FT-IR Spectroelectrochemistry Studies on the Electrochemical Redox Process. *J. Phy. Chem. B* **2007**, *111*, 1517−1522.
(38) Bard, A. J.; Faulkner, L. R. *Electrochemical Methods: Fundamentals and Applications*; John Wiley and Sons: New York, 2001.
(39) Ossowski, T.; Pipka, P.; Liwo, A.; Jeziorek, D. Electrochemical and UV-Spectrophotometric Study of Oxygen and Superoxide Anion Radical Interaction with Anthraquinone Derivatives and Their Radical Anions. *Electrochim. Acta* **2000**, *45*, 3581−3587.